Biochimica et Biophysica Acta, 1026 (1990) 225–235
Elsevier

BBAMEM 74916

Comparisons of lipid dynamics and packing in fully interdigitated monoarachidoylphosphatidylcholine and non-interdigitated dipalmitoylphosphatidylcholine bilayers: cross polarization/magic angle spinning ^{13}C-NMR studies

Wen-guey Wu and Lang-Ming Chi

Institute of Life Sciences, National Tsing Hua University, Hsinchu, Taiwan (China)

(Received 29 January 1990)
(Revised manuscript received 21 March 1990)

Key words: Dipalmitoylphosphatidylcholine; Lysophosphatidylcholine; Interdigitated bilayer; NMR; Cross polarization/magic angle spinning; DSC

^{13}C-NMR spectra have been obtained at 50.3 MHz for monoarachidoylphosphatidylcholine (MAPC) and dipalmitoylphosphatidylcholine (DPPC) dispersions from 25 °C to 55 °C and for DPPC polycrystals at 25 °C using the cross polarization/magic angle spinning technique. Differential scanning calorimetric studies on DPPC and MAPC dispersions show comparable lipid phase transitions with transition temperatures at 41 °C and 45 °C, respectively, and thus enable the comparison of thermal, structural and dynamic differences between these two systems at corresponding temperatures. Conformational-dependent ^{13}C chemical shift studies on DPPC dispersions demonstrate not only the coexistence of the tilted gel ($L_{\beta'}$) and liquid-crystalline (L_α) phases in the rippled gel ($P_{\beta'}$) phase, but also the presence of an intermediate third microscopic phase as evidenced by three resolvable peaks for $\omega - 1$ methylene carbon signals at the temperature interval between T_p and T_m. By comparing chemical shifts of MAPC in the hydrocarbon chain region with those of DPPC at similar reduced temperatures, it can be concluded that the packings are perturbed markedly in the middle segment of the fatty acyl chain during the lamellar to micellar transition. However, terminal methylene and methyl groups of interdigitated MAPC lamellae were found to be more ordered than those of non-interdigitated DPPC bilayers in the gel state. Interestingly, the terminal methyl groups of MAPC in the micelles remain to be relatively ordered; in fact, they are more ordered than the corresponding acyl chain end of DPPC in the liquid-crystalline state. Analysis of data obtained from rotating frame proton spin-lattice relaxation measurements shows a highly mobile phosphocholine headgroup, a rigid carbonyl group and an ordered hydrocarbon chain for lamellar MAPC in the interdigitated state. Furthermore, results suggest that free rotations of the glycerol C2–C3 bond within MAPC molecules may occur in the interdigitated bilayer, whereas intramolecular exchange between two conformations of the glycerol backbone in DPPC become possible at temperatures close to the pretransition temperature. Without isotope enrichment, we conclude that high-resolution solid-state ^{13}C-NMR is indeed a useful technique which can be employed to study the packing and dynamics of phospholipids.

Introduction

It has been well established that lysophosphatidylcholine molecules can aggregate to form extended lamellar structures in excess water if they are allowed to incubate at temperatures well below the lamellar to micellar thermal transition temperature (T_m) for an extended period [1,2]. Evidence in support of the full interdigitation of lysophosphatidylcholine, i.e., the long acyl hydrocarbon chain extends across the entire hydro-

Abbreviations: CP/MAS, cross polarization/magic angle spinning; NMR, nuclear magnetic resonance; MAPC, monoarachidoylphosphatidylcholine; MSPC, monostearoylphosphatidylcholine; MPPC, monopalmitoylphosphatidylcholine; DPPC, dipalmitoylphosphatidylcholine; DMPC, dimyristoylphosphatidylcholine; DLPC, dilauroylphosphatidylcholine; $T_{1\rho}$, rotating frame proton spin-lattice relaxation time; DSC, differential scanning calorimetry; TMS, tetramethylsilane.

Correspondence: W. Wu, Institute of Life Sciences, National Tsing Hua University, Hsinchu, Taiwan 30043, China.

carbon width of the bilayer, was provided by data from X-ray determination of the bilayer thickness and the average surface area at the lipid/water interface [3,4]. Recently, other interdigitated bilayer systems have been observed for lipids under a wide variety of physical and chemical conditions (for reviews see Refs. 5 and 6). The structures of these interdigitated bilayers vary from the partially interdigitated, mixed interdigitated, to fully interdigitated lamellae, depending on the temperature, pressure, lipid compositions and inducing agents. The interdigitated hydrocarbon chains in these systems were found primarily at $T < T_m$, or in the ordered *gel state* bilayers [7,8]. Although it is now commonly accepted that a substantial part of the lipid species in biological membranes exists in the *fluid state,* membranes are capable of forming domains in which lipids in both the fluid and gel states can coexist in equilibrium in normal bilayers [9] or even in the interdigitated bilayer [10]. Therefore, it is of biological interest to study the physical properties of interdigitated gel-phase bilayers.

Dipalmitoylphosphatidylcholine (DPPC) dispersed in excess water can self-assemble into non-interdigitated bilayers, which have been extensively studied as model membranes. These fully hydrated DPPC molecules in non-interdigitated bilayers are known to undergo multiple phase transitions as detected by various physical techniques [11–13]. Based on X-ray scattering patterns obtained from unoriented samples, the phase transition at approx. 41°C, the so-called main phase transition temperature (T_m), can be attributed primarily to the order-disorder melting of the hydrocarbon chain [14], and the broad, low enthalpy pretransition at approx. 35°C (T_p) can be associated with the change of lipid molecules in a one-dimensional ordered $L_{\beta'}$ phase into a two-dimensional ripple $P_{\beta'}$ phase [15]. Solid-state ^{13}C nuclear magnetic resonance (NMR) studies of ^{13}C-labeling at the carbonyl position of the *sn*-2 chain of DPPC molecules provide further evidence suggesting that DPPC in the $P_{\beta'}$ phase at temperatures between T_p and T_m exhibits structural and dynamic properties of both the ordered $L_{\beta'}$ phase and the disordered L_α phase [16,17]. Since the cross polarization/magic angle spinning (CP/MAS) technique can now be performed to obtain high-resolution ^{13}C-NMR spectra of multilamellar liposomes [18], it was of interest for us to apply the CP/MAS ^{13}C-NMR technique to study the dynamics as well as the molecular packing of interdigitated bilayer systems. A comparison of the dynamic properties exhibited by interdigitated bilayers with those of DPPC lamellae, which have not been fully explored using the CP/MAS technique, should shed more light on the lipid–lipid interactions in these two different bilayer systems.

The present study will first show that aqueous dispersions of monoarachidoylphosphatidylcholine (MAPC), a lysophospholipid molecule with a hydrocarbon chain length of C_{20}, can undergo a lamellar to micellar phase transition with a transition temperature of approx. 45°C. This phase transition temperature is comparable to the T_m of DPPC dispersions. Comparative studies of the interdigitated and the non-interdigitated bilayer prepared from MAPC and DPPC, respectively, using data derived from conformational-dependent ^{13}C chemical shift and its rotating frame proton spin-lattice relaxation time ($T_{1\rho}$) are presented in this communication. These results provide new information on the dynamics and packings of lipids in the interdigitated and non-interdigitated bilayer systems.

Materials and Methods

Dipalmitoylphosphatidylcholine (DPPC) and monoarachidoylphosphatidylcholine (MAPC) were obtained from Avanti Polar Lipids, Inc. AL, U.S.A. DPPC polycrystals were recrystalized from a water-containing solution [19] and were seen under the polarized light microsocpe to be microcrystal aggregates. Multilamellar dispersions of normal and interdigitated bilayers of DPPC and MAPC, respectively, were prepared first by adding an excess of doubly distilled H_2O at room temperature and then the samples were cycled through 45°C three times. Samples were incubated at room temperature overnight and packed by centrifugation. They were finally transferred to either ZrO_2 rotors for CP/MAS ^{13}C-NMR or an aluminum pan for differential scanning calorimetry (DSC) studies. ^{13}C-NMR spectra were obtained at 50.3 MHz with a Brüker-MSL 200 NMR spectrometer capable of high-power ^1H decoupling, ^1H–^{13}C cross polarization and magic angle spinning. The spinning rate varied typically in the range of 1.5–2.5 kHz depending on the temperatures, which might affect the spinning of the Andrew-type rotor due to the packing properties of the liposomes in the rotor. Rotating frame proton relaxation time, $T_{1\rho}$, measurements were performed by varying the contact time in the cross polarization pulse sequence [20]. The intensities of spectra were then simulated according to Eqn. 1.

$$I(t_c) = I(0)\, e^{-t_c/T_{1\rho}}[1 - e^{-t_c(1/T_{HC} - 1/T_{1\rho})}] \quad (1)$$

where t_c is the time of dipolar contact, T_{HC} is the cross polarization time constant and $T_{1\rho}$ is the spin-lattice relaxation time in the rotating frame of the proton reservoir [21]. All spectra were referenced to an external standard of tetramethylsilane (TMS) and high-frequency, low-field shifts are denoted as positive. All DSC experiments were performed with a DuPont 910 DSC system. The calorimeter was interfaced to a DuPont Thermal Analyst 2100 system for automatic data collection and analysis. A scan rate of 0.5 C° per min was used in the ascending temperature mode ranging from 23°C to 55°C. Enthalpy measurements were

TABLE I

Thermodynamic properties of monoacylphosphatidylcholine dispersions

Chain length	T_m (°C)	$\Delta T_{1/2}$ (C°)	ΔH (kcal/mol)	ΔS (e.u./mol)
MPPC (C_{16})	3.5	0.3	4.6	16.6
MSPC (C_{18})	26.2	0.5	7.0	23.4
MAPC (C_{20})	45	6	8.5	26.7

determined from the area under the transition peak by comparison with that of known standard (indium). Phospholipid concentrations were determined as inorganic phosphorus by the method of Bartlett [22].

Results

DSC experiments

Representative DSC heating thermographs for MAPC and DPPC dispersions are shown in Fig. 1. The main endothermic transitions for DPPC and MAPC dispersions are peaked at 41° C and 45° C, respectively. The transition temperature (T_m), transition enthalpy (ΔH), half-height width ($\Delta T_{1/2}$) and transition entropy (ΔS) for a homologous series of lysophosphatidylcholines in excess water are summarized in Table I. Systematic changes in both T_m and ΔH for these lysolipid dispersions suggest strongly that they all undergo a lamellar to micellar thermal transition as reported previously [7,23].

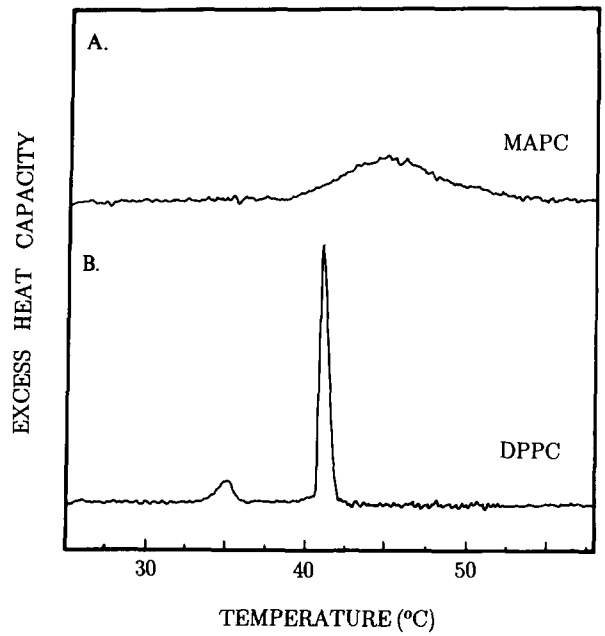

Fig. 1. DSC traces of aqueous multilamellar dispersions of (A) MAPC and (B) DPPC for a heating scanning rate of 0.5 C°/min. Repeated scans of samples incubated at room temperature for 4 h showed the same scanning profiles.

Chemical shift data

The upper and middle traces of Fig. 2 show the expanded high-resolution ^{13}C-NMR spectra of fully hydrated DPPC multilamellar dispersions at 30° C and

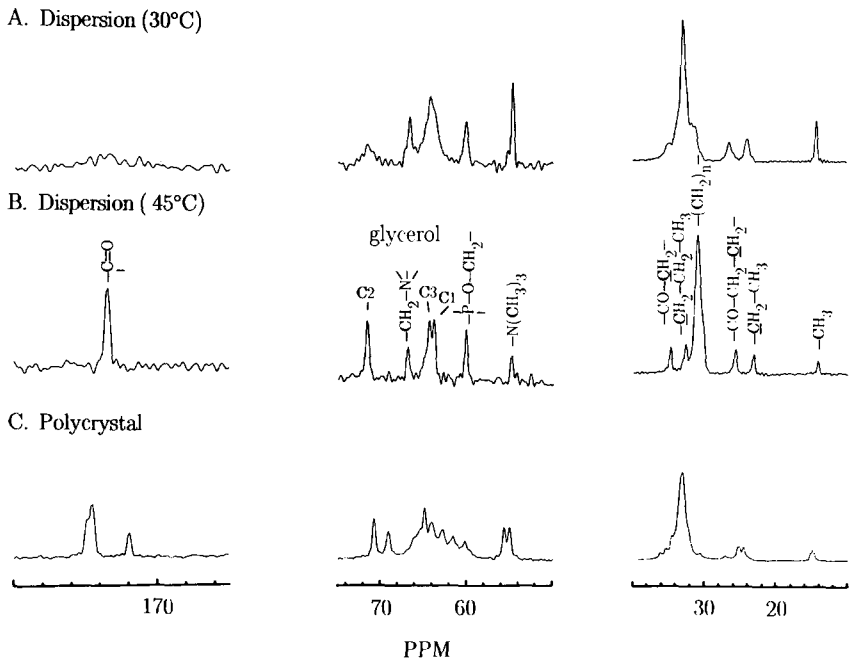

Fig. 2. CP/MAS 50.3 MHz ^{13}C spectra of DPPC in: (A) fully hydrated dispersions at 30° C, (B) fully hydrated dispersions at 45° C, and (C) polycrystals at 25° C. Contact times for polarization are 2 ms. Chemical shifts are relative to TMS. Note that the scales and intensities of each spectrum in three regions are different.

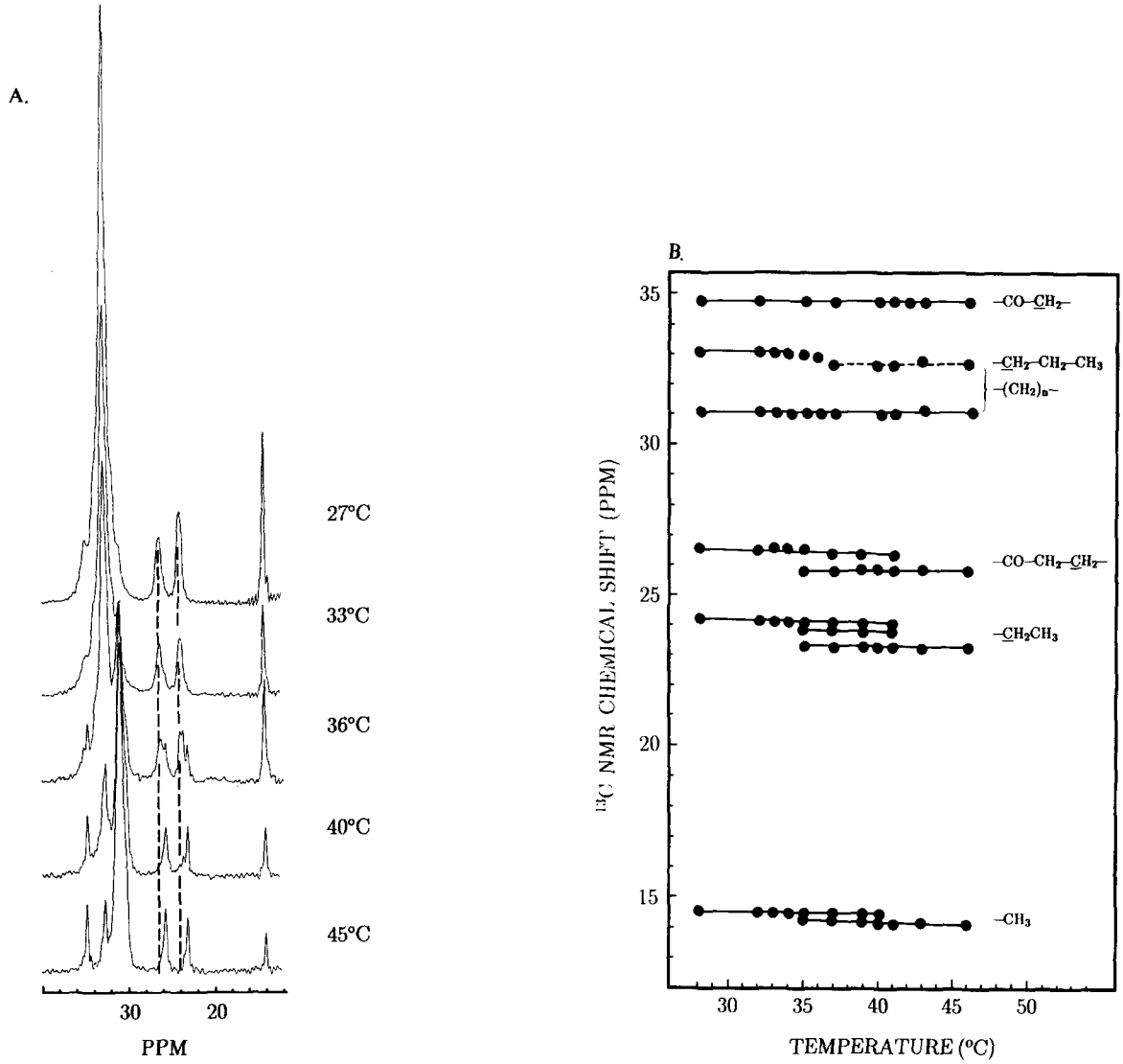

Fig. 3. (A) Representative temperature-dependent ^{13}C spectra for the fatty acyl chain of DPPC. (B) Chemical shifts of ^{13}C-NMR spectra plotted as a function of temperature. Each spectrum was typically 1000 scans with a 1.5 s delay time, 4 μs 90 degree pulse and 2 ms contact time. Two dashed vertical lines are plotted to emphasize the effect of temperature on the resonance positions of β and $\omega - 1$ carbons of the fatty acyl chain in the $L_{\beta'}$ phase.

45 °C, respectively. In the same figure (lower traces), spectra of DPPC polycrystals recorded at 25 °C are included for comparison. The assignments of ^{13}C peaks for fully hydrated DPPC were first made according to Burns and Roberts [24]. For aqueous dispersions of DPPC, six well-resolved ^{13}C-peaks can be assigned to phosphocholine and glycerol carbons (the middle trace). There are, however, a minimum of nine discernible ^{13}C-peaks for DPPC polycrystals recorded in the same region. This result is consistent with previous X-ray single crystal studies, indicating that there are more than one conformation of phosphatidylcholine molecules [19]. Major differences between gel-state (30 °C) and fluid-state (45 °C) spectra of DPPC can be detected in the hydrocarbon chain region. The most intense peaks at 31.0 or 33.1 ppm correspond to the methylene groups in the fatty acyl chain. This resonance was shifted from 33.1 ppm to 31.0 ppm as the temperature of the sample was increased from 30 °C to 45 °C. Since major polymethylene resonances for all-*trans* fatty acyl chain of DPPC polycrystlas were detected at 33.5 ppm (with shoulders at 34 ppm), the upfield shifts of fatty acyl chain upon hydration and heating must be due to the *trans-gauche* isomerization and lateral expansion of phospholipids in the bilayers [25,26]. The influence of lipid dynamics and packing on ^{13}C-NMR chemical shifts can also be found in other methylene peaks from both ends of the fatty acyl chain. This was evidenced by systematic studies of the effect of temperature on the chemical shifts of all resolvable resonances in this region. Fig. 3A shows representative ^{13}C-NMR spectra of such studies; the change of the ^{13}C chemical shift as a

TABLE II

^{13}C-NMR chemical shifts (ppm relative to TMS) of monoacyl- and diacylphosphatidylcholine multilamellar bilayers or micelles obtained using the CP/MAS technique

Carbon atoms	DPPC		MAPC	
	28 °C	46 °C	33 °C	50 °C
Headgroup				
CH_2N (Cβ)	66.7	66.8	66.7	66.9
CH_2OP (Cα)	60.1	60.1	60.1	60.2
$N(CH_3)_3$ (Cγ)	54.8	54.8	54.8	54.9
Backbone				
CHO (C-2)	71.5	71.5	69.1	69.3
CH_2OP (C-3)	64.4	64.4	67.5	67.6
CH_2O (C-1)	63.8	63.8	66.1	66.2
Carbonyl	173.8	173.6	174.1	174.1
Alkyl				
$-(CH_2)_n-$	33.1	31.0	33.4	30.6
α	34.7	34.7	34.6	34.6
β	26.5	25.8	26.3	25.5
ω − 1	24.2	23.2	24.7	23.2
ω	14.5	14.2	15.0	14.5

function of temperature is plotted in Fig. 3B. It is clear that ^{13}C resonance positions for the hydrocarbon chain from the $L_{\beta'}$ and L_α phases are distinctively different. Interestingly, DPPC in the $P_{\beta'}$ phase or the temperature range between T_p and T_m exhibits superpositions of at least two peaks, indicating the coexistence of microscopic structural properties of both the $L_{\beta'}$ and L_α phases. A similar conclusion has been drawn according to ^{13}C-labeled solid-state NMR studies [16]. The ω − 1 methylene resonances show three resolvable peaks (see the 36 °C spectrum in Fig. 3A), indicating the complexity of lipid acyl chains in the ripple phase. It should be mentioned that there is no detectable chemical shift change for polar phosphocholine headgroup resonances at the temperature range studied (data not shown, see also Fig. 1). At the interfacial glycerol backbone region, ^{13}C-NMR signals were detected to be broadened at temperatures slightly below T_p. The significance of these broadening effects on glycerol resonances at $T < T_m$ will be discussed later.

The aforementioned results obtained from DPPC can now be used for comparison with results obtained from MAPC. Fig. 4A shows representative hydrocarbon chain ^{13}C-NMR spectra of MAPC at the indicated temperatures, and Fig. 4B illustrates the temperature dependence for each ^{13}C chemical shift parameter. Since the half-height of DSC peaks for MAPC are quite broad (6 C°), one can examine the process of chain melting at the phase transition temperature. Phase separation of MAPC lipid aggregates can clearly be seen as judged from the coexistence of two resonances displayed by the hydrocarbon chain. The difference between chemical shifts obtained at temperatures above and below the phase transition, or micellar and lamellar phases, in general, were greater than that of DPPC recorded at

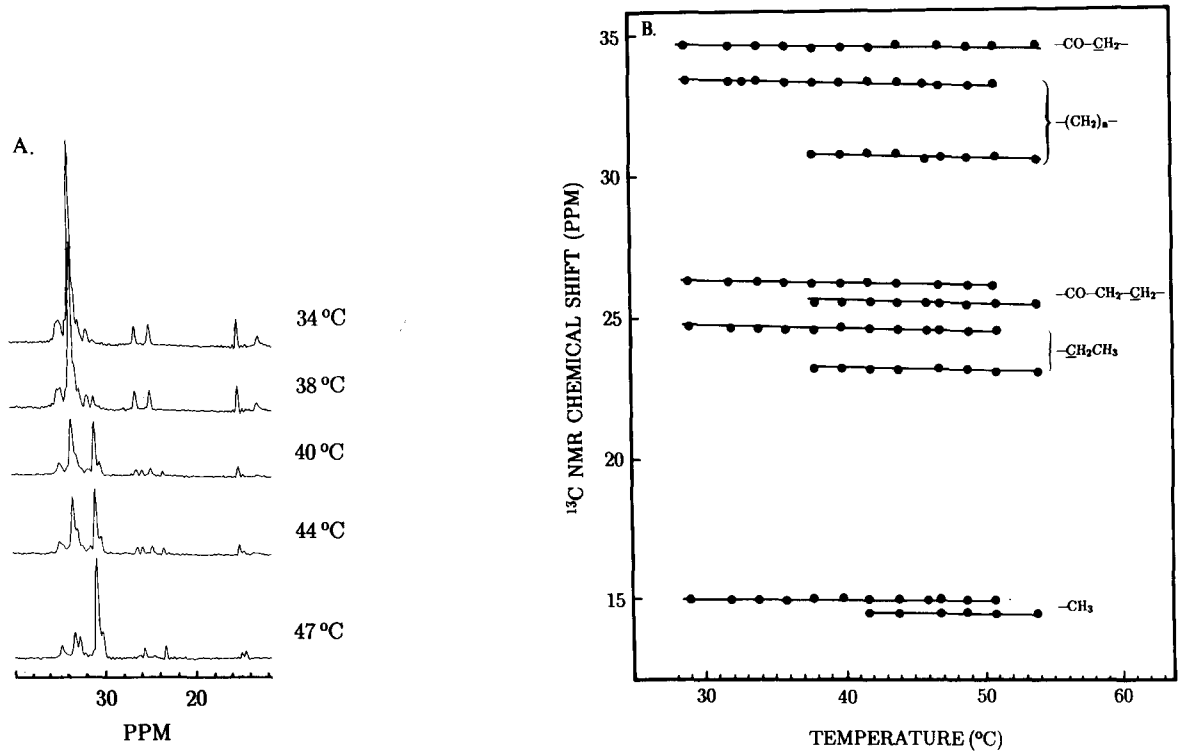

Fig. 4. (A) Representative temperature-dependent ^{13}C spectra for the fatty acyl chain of MAPC. (B) Chemical shift dependence as a function of temperature.

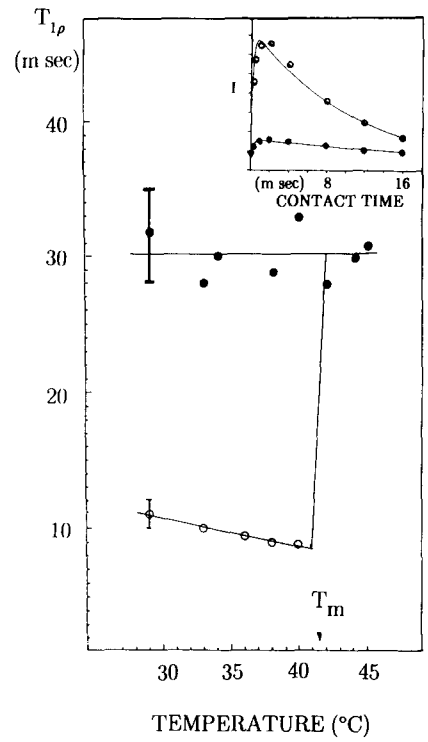

Fig. 5. $T_{1\rho}$ of the proton reservoir as a function of temperature for two resonances of the fatty acyl chain in $L_{\beta'}$ (33 ppm; ○) and L_{α} phase (31 ppm; ●) of DPPC bilayers. Note that two phases coexist for temperatures below T_m. These values were determined by least-square fitting according to Eqn. 1 (see text). Examples of fitting are shown in the upper right panel, where signal intensities are plotted as a function of contact time.

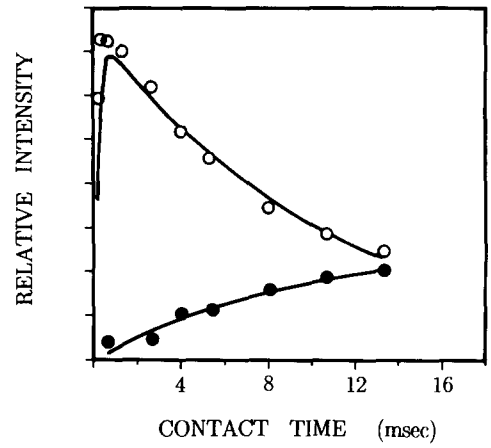

Fig. 6. Signal intensities of ^{13}C-NMR spectra for MAPC dispersion at 45° C plotted as a function of dipolar contact time. Peaks of 33.4 ppm (○) and 30.0 ppm (●) were chosen to represent the hydrocarbon chain signal of interdigitated bilayers and micelles, respectively.

corresponding temperatures. For future reference and discussion, the values of chemical shifts from these two lipids systems are summarized in Table II.

Rotating frame relaxation measurements

The $T_{1\rho}$ values determined by the varying contact time for two coexisting methylene resonances of DPPC are plotted in Fig. 5 as a function of temperature. The high-field resonances (31.0 ppm) show larger $T_{1\rho}$ values of 30 ms, whereas low-field resonances (33.1 ppm) show

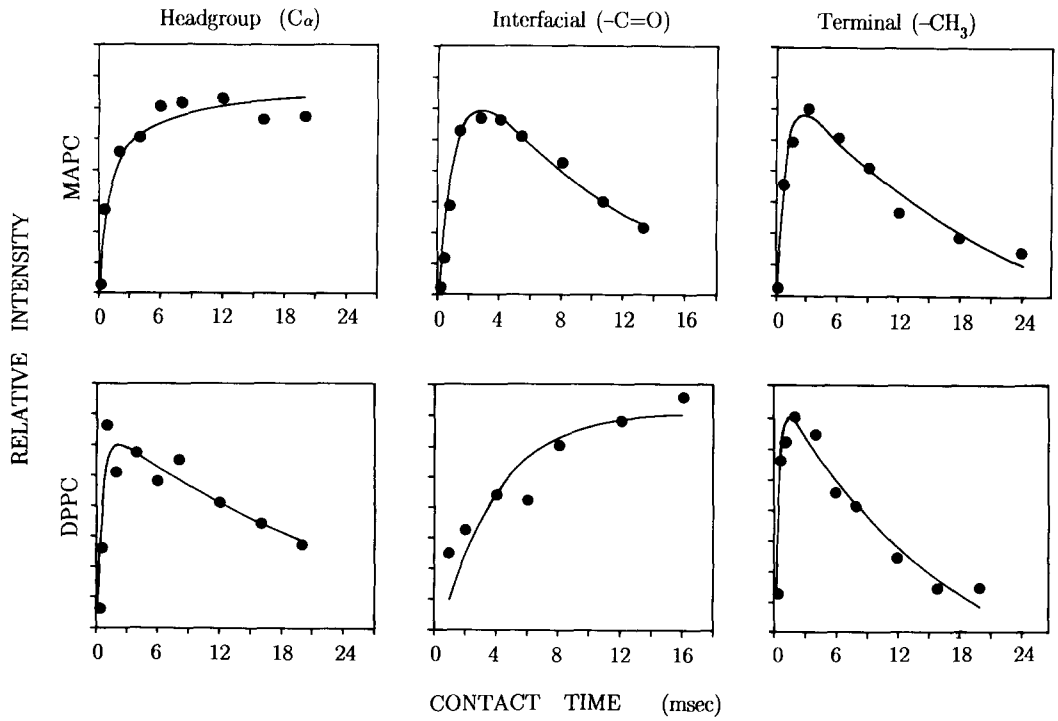

Fig. 7. Variation of integrated intensities of peaks from ^{13}C-NMR spectra of MAPC (upper panel) and DPPC (lower panel). The solid lines were obtained by least-square fitting according to Eqn. 1.

smaller $T_{1\rho}$ values of 10 ms. Thus relaxation measurements confirm our conclusion, drawn from chemical shift data, that changes in the ^{13}C chemical shift result from changes in lipid dynamics. Further quantitative interpretation of $T_{1\rho}$ data will be discussed below. It should be mentioned here that the determination of the $T_{1\rho}$ value is not possible for highly fluid sample such as micelles. Fig. 6 illustrates an example of such a measurement of MAPC at 45 °C, where a phase separation would occur during the melting process. Depite that the ^{13}C-NMR resonance at 33.4 ppm shows a single exponential $T_{1\rho}$ relaxation, the other peak at 30.6 ppm exhibits no sign of decay from 0.2 ms to 20 ms contact time. In fact, as long as MAPC micelles remain in the fluid state, intensities of all peaks from ^{13}C-NMR spectra would exhibit long T_{HC} with no measurable $T_{1\rho}$. Similar behavior has also been found for peaks of phosphocholine polar headgroup from DPPC bilayers in the fluid state. At temperatures well below the lipid phase transition, however, interesting contrasts were found for MAPC interdigitated and DPPC non-interdigitated bilayers. Shown in Fig. 7 are variations of signal intensity as a function of contact time for ^{13}C-NMR peaks from CH_2OP of phosphocholine, C=O of carbonyl group and $-CH_3$ of the terminal hydrocarbon chain for MAPC (36 °C) and DPPC (32 °C) at similar reduced temperatures. Terminal methyl groups from both interdigitated and non-interdigitated bilayers show similar $T_{1\rho}$ values of 18 ± 1 ms in the gel state. However, under the same experimental condition, no measurable $T_{1\rho}$ relaxation decay can be detected for the phosphocholine headgroup of MAPC and the interfacial carbonyl group of DPPC bilayers. In contrast, the phosphocholine headgroup of DPPC and the interfacial carbonyl group of MAPC show $T_{1\rho}$ values of 18 ms and 35 ms, respectively.

Discussion

The conformational-dependent ^{13}C chemical shift obtained by high-resolution solid-state ^{13}C-NMR has recently been used as a new approach for conformational characterization of biological macromolecules such as carbohydrates and proteins [27]. Magic angle spinning ^{13}C-NMR studies on isotopically labeled retinal and rhodopsin have also provided detailed molecular information about the structure and function of light-transducing proteins [28]. In addition, Oldfield and coworkers [18] demonstrate that lipid molecules such as cholesterol in multilamellar liposomes can be observed in magic angle spinning NMR spectra, which are not observable in sonicated model membrane systems. Despite the above-mentioned advantage, the application of this technique to the study of model and biological membranes seems not to be as popular as other solid state techniques such as ^{2}H-NMR [29–31]. In this communication, we present our studies on the structure and dynamics of lipids using the CP/MAS technique without isotope enrichment. Specifically, we investigate the structures and dynamics of DPPC in polycrystals and dispersions and compare them in the different physical packing states of the L_α, $P_{\beta'}$ and $L_{\beta'}$ phases. Lipid packing and dynamic properties of MAPC in interdigitated bilayer and in micelles were also studied by comparison with those of DPPC in non-interdigitated bilayers at similar reduced temperatures. Our data obtained from DPPC studies confirmed several conclusions made previously using other techniques. For instance, from previous DMPC single-crystal studies [19], the unit cell of DMPC is known to contain two lipid molecules with A and B conformations. These two conformations differ mainly in their torsion angles in the polar headgroup. Our results shown in Fig. 2 demonstrate that ^{13}C-NMR spectra obtained from DPPC polycrystals were superimposed spectra from more than one conformation. Although at the present time we are not able to assign peaks from DPPC polycrystals or to deduce structure information from ^{13}C chemical shifts, this result clearly shows that CP/MAS ^{13}C-NMR is a powerful technique for comparison of structures in different physical states. Studies on the ^{13}C-labeled DPPC have shown that the $P_{\beta'}$ phase of DPPC exhibits microscopic structural and dynamic properties of both the ordered $L_{\beta'}$ and disordered L_α phase. Our results shown in Fig. 3 also show that, at $\omega - 1$ hydrocarbon position, not only a superposition of these two phases coexists, but also that the other intermediate $P_{\beta'}$ phase can be detected. Since the $P_{\beta'}$ phase and crystal structures have been extensively studied previously [32,33], we will not discuss these issues further. The following discussions will mainly focus on the thermodynamic and structural properties of MAPC.

Lamellar to micellar transition of MAPC

In the presence of excess water, lipid assemblies of a variety of synthetic diacylphosphatidylcholines are known to undergo bilayer gel ↔ liquid-crystalline phase transition. Fully hydrated dispersions of monopalmitoylphosphatidylcholine (MPPC), monostearoylphosphatidylcholine (MSPC) and *n*-octadecylphosphocholine have been shown to self-assemble at $T < T_m$ into a highly ordered two-dimensional lamellar organization in which the acyl chains are fully interdigitated [2,7,23]. This interdigitated gel phase transforms into the micellar phase upon heating at a characteristic phase transition temperature. The present study demonstrates that fully hydrated MAPC molecules also exhibit a thermal transition at a transition temperature of 45 °C with a half-width of 6 C° and a transition enthalpy of 8.5 kcal/mol. As can be seen from Table I, not only the transition temperature and enthalpy increase as a result of a longer hydrocarbon chain, but also the half-width

of lipid phase transition increases significantly. The purity of MAPC has been checked using thin-layer chromatography and found to be better than 99% and, thus, the half-width of its phase transition cannot be due to lipid impurity. One way of accounting for the wide range of MAPC melting temperatures is to attribute it to the heterogeneity of the micellar structure above the phase transition. The size distribution of MAPC micelles was found to be quite heterogeneous (from approx. 40 Å to more than 500 Å) as judged by Sepharose CL-4B molecular sieve chromatographic and quasielastic light-scattering studies [34]. Other shorter-chain lysophospholipids such as MSPC, however, show a monodispersed size distribution in the concentration range 0.01–100 mM. Transitions of multilamellar structures into micelle suspensions with different aggregation numbers should exhibit different thermodynamic properties, since the molecular interaction potentials were different in these aggregated states. In fact, the liposomal size has been demonstrated to limit the cooperativity of the phospholipid phase transition using high sensitivity DSC [46]. Since only one type of the ^{13}C-NMR resonances was detected for micellar phases (see Fig. 4), the hydrocarbon packing of the putative MAPC micelles with different aggregation numbers should be similar.

Lipid packing in interdigitated gel state bilayers and fluid state micelles

Based on the relative magnitude of the Raman peak/height intensity ratio, it has been concluded that MSPC are packed in a more orderly fashion than distearoylphosphatidylcholine at temperatures below T_m, but they are very disordered at temperatures above T_m [7]. A similar but more specific conlusion can be drawn if a comparison is made between differences in the chemical shifts obtained above and below the phase transition temperature for aqueous dispersions of MAPC and DPPC. These comparisons can be made in two ways. First, as shown in Fig. 3B and Fig. 4B, the chemical shift differences below and above the lipid phase transition are larger for MAPC than for DPPC. It is known that ^{13}C resonances of alkane hydrocarbons will shift upfield up to 5 ppm when a γ methyl is brought into juxtaposition with the methylene by *gauche* conformation of the intervening α–β bond [37]. This observation provides a simple way of monitoring the populations of *gauche* vs. *trans* rotamers of phospholipids in terms of ^{13}C-NMR chemicals shift. Generally speaking, the upper field signals (e.g., 31, 25.8 and 23.3 ppm) represent resonances from the liquid state with more *gauche* rotamers and the lower field signals (e.g., 33, 26.5 and 24.2 ppm) represent those from the gel states with most *trans* rotamers. Therefore, changes in lipid packing, as reflected by the *trans* to *gauche* ratio are larger for MAPC than for DPPC on lipid phase

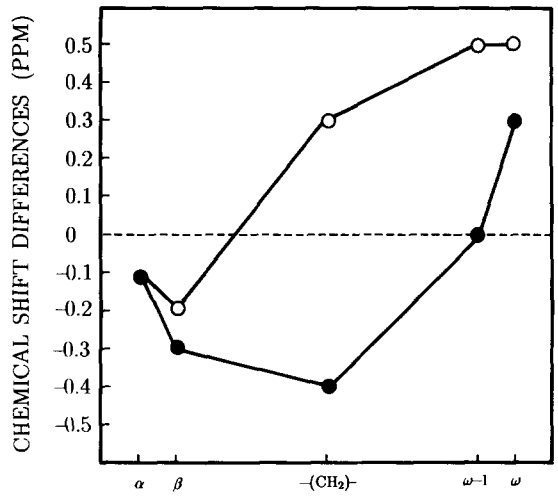

Fig. 8. Differences of the ^{13}C-NMR chemical shift values between MAPC and DPPC dispersions at similar reduced temperatures above (●; T_m+5 C°) and below (○; T_m-12 C°) lipid thermal phase transitions.

transition. Second, more specific information can be obtained if we compare MAPC with DPPC (Fig. 8) at the same reduced temperatures. For instance, in the gel state, the ω and the $\omega-1$ positions of the alkyl chain were shifted, relative to the non-interdigitated bilayer, to a low-field position by 0.5 ppm (the largest shift for all hydrocarbon resonances; see Table II), indicating that terminal hydrocarbon chains locked between two lipid molecules become highly ordered. For fully interdigitated bilayers of monoacylposphatidylcholine to be stable, it is essential that the terminal alkyl group remain in an ordered state so that the surface area of the phosphatidylcholine (PC) molecules at the water/lipid interface can be maintained at approx. 45 Å^2 [3]. We thus provide the first CP/MAS NMR spectroscopic evidence that the conformation of the chain terminal methyl group of monoacyl PC is, indeed, quite different from that of diacyl PC. In the fluid state, another interesting observation can be made. Subtracting ^{13}C-NMR chemical shifts of alkyl hydrocarbons in column 3 (DPPC at 46 °C) of Table II from those in column 5 (MAPC at 50 °C), values of −0.1 ppm, −0.3 ppm, −0.4 ppm, 0 ppm and +0.3 ppm can be obtained for α, β, -(CH_2)-, $\omega-1$, and ω carbons, respectively. These values are plotted in Fig. 8 as a function of the hydrocarbon position in either gel state, i.e., interdigitated vs. non-interdigitated, or fluid state, i.e., bilayer vs. micelles. Reversal of the sign of the chemical shift from 0.3 ppm to −0.4 ppm suggests that the packing of the hydrocarbon chain in micelles is most perturbed in the middle part of the fatty acyl chain. Interestingly, at the terminal methyl group, MAPC micelles still remain in a relatively more ordered state than DPPC bilayers. We must emphasize that the perturbed packing in the

middle part of hydrocarbon chain and the ordered structure in the terminal methyl group for monoacyl PC micelles are only relative to the packing of DPPC molecules in the bilayer structure. This does not necessarily increase the order parameters of the methylene group when going down the hydrocarbon chain as proposed previously by Dill and Flory [38]. The order parameters for anisotropic phases, such as lipid bilayers, have been obtained from deuterium molecules. A flexibility gradient along the center of the bilayer (those near the terminal methyl group) and a plateau with an approximately constant value of order parameters were observed in saturated diacyl PC bilayers [39]. Similar profiles for several detergent micellar systems were also detected by ^{13}C-NMR spin-lattice relaxation and nuclear Overhauser effect studies [40]. In the micellar studies, which are more relevant to our results, it was found that the so-called 'plateau' region in the order parameter profiles could be greatly reduced if the temperature of the studied system was raised. We interrelated a large chemical shift change in the middle part of the hydrocarbon chain as an indication of the reduced order parameter plateau in micelles. Therefore, our results are consistent with other relaxation studies [40]. The idea that the order parameter near the terminal end of the hydrocarbon chain in micelles could be reversed might in someway be reflected in our data, as shown in Fig. 8. The magnitude of this reversed order packing is simply not large enough to be detected as changes of order parameters.

Comparison of lipid dynamics between interdigitated and non-interdigitated bilayers

In this section, we will mainly discuss the results of our rotating frame relaxation measurements and the broadened linewidth of the ^{13}C-NMR signal from glycerol carbons at temperature close to pretransition. Boroske and Trahms [21] have investigated motional changes of DPPC molecules associated with the pretransition in multilamellar bilayers by proton-enhanced ^{13}C-NMR and spin-locking experiments. In the present study, we also measured $T_{1\rho}$ as a function of temperature for DPPC bilayer (Fig. 5) by also using the magic angle spiing (MAS) technique. Without MAS, studies using low-resolution ^{13}C-NMR spectra in the gel state would obtain obscured $T_{1\rho}$ values for the fatty acyl hydrocarbon chain, since it has been shown (Fig. 3) that both the disordered and ordered states of hydrocarbon chains coexist in the gel state at temperatures far below the main lipid phase transition temperature. Our data, however, are consistent with previous results in the qualitative aspect that the $T_{1\rho}$ value is smaller in the gel state and larger in the fluid state. It should be mentioned that our $T_{1\rho}$ measurements were performed at an approx. 40 kHz proton locking field with a spectrometer operating at a 50 MHz ^{13}C resonance. For an estimation of τ_c one may assume the time constant, $T_{1\rho}(\tau_c)$, according to Eqn. 2, to have its minimum at $\tau_c = (2\omega_1)^{-1}$,

$$T_{1\rho}^{-1} \propto \tau_c/(1+4\omega_1^2\tau_c^2) \quad (2)$$

where $\omega_1 = \gamma H_{1H}$ is the Zeeman frequency of the proton spins with respect to the rotating field, H_{1H} [21]. Judging from the temperature-dependent profile of the $T_{1\rho}$ value for gel state hydrocarbon chain resonances, i.e., $T_{1\rho}$ decreases slightly when temperature increases, one can reasonably assume that the $T_{1\rho}$ value determined is close to its minimum. Taking an experiment value of $\omega_1 \simeq 40$ kHz, one can calculate τ_c to be 10^{-5} s. The molecular motion of DPPC bilayers in the gel state has been studied by electron spin resonance measurements [41]. The effective correlation time of approx. 10^{-6} s is detected at a temperature close to the pretransition onset temperature. Our estimated correlation time is consistent with that of the $L_{\beta'}$ phase determined by electron spin-resonance saturation transfer experiments.

As shown in Fig. 6, determination of the $T_{1\rho}$ value for fluid state micelles is not possible, because its intensity did not show any detectable decay in the experimental time range. However, the relatively small cross polarization efficiency, long T_{HC} and no measurable $T_{1\rho}$ for the intensity profile measured for the liquid hydrocarbon chain at 31 ppm suggest a pattern of the 'fluid state' rotating frame relaxation. This can be seen clearly in Fig. 7, where C_α of phosphocholine from MAPC in the interdigitated bilayer shows an intensity-contact time profile similar to that for the high mobility carbon signals. It has been shown by ^{31}P- and ^{2}H-NMR that ether-linked phosphatidylcholines, such as dihexadecyl PC (DHPC), show the presistence of long-axis diffusion to much lower temperatures in the interdigitated gel phase of DHPC than in the non-interdigitated gel phase of DPPC [42,43]. Our CP/MAS ^{13}C-NMR data also suggest high mobility of the phosphocholine headgroup in the interdigitated gel state bilayers. However, in our case high mobility of the headgroup for monoacyl PC is not due to the fast long-axis diffusion of lipid molecules proposed for DHPC. $T_{1\rho}$ relaxation at other regions of the carbon signal, such as terminal methyl and fatty acyl chain, indicate the highly ordered structure of MAPC. We believe that the fast mobility of the monoacyl PC headgroup is due to the free rotation of the C2–C3 bond of the glycerol moiety as suggested previously [44]. Both the chemical shift anisotropy of ^{31}P-NMR and the quadrupolar splitting of ^{14}N-NMR were reduced by a factor of two for monoacyllysophospholipids in comparison with diacylphospholipids. It can be concluded that the high mobility of monoacylphospholipids is only restricted to the headgroup of interdigitated PC molecules.

The structures and dynamics properties of phospholipid molecules in the interfacial region of bilayers is

most interesting, since it plays a crucial role in monitoring the packing of the hydrocarbon chain and in determining the conformation of the headgroup. For instance, conformational change at the glycerol backbone has been detected by broad-line ^{13}C-NMR above and below the lipid phase transition. Specifically, the glycerol backbond in the gel state is in a *gauche* conformation, while in the fluid phase a different conformation is preferred for dipalmitoylphosphoethanolamine [45]. In our high-resolution ^{13}C-NMR spectra, we found that the linewidths for three glycerol carbons and carbonyl group were significantly broadened relative to other phosphocholine carbons in the same samples (Fig. 2). The broadened linewidth at $T < T_m$ is interpreted as a result of intramolecular nuclear spin exchange in the glycerol region within the lipid molecule itself. Although the exact conformation of the two putative types of structure undergoing exchange is not clear. It is reasonable for us to assume that they were the two structures detected in our CP/MAS ^{13}C-NMR spectra (Fig. 2). Unfortunately, we are not able to assign specifically the resonances obtained from polycrystal samples at the present time. A rough estimation of the exchange rate, however, can still be obtained. Judging from the peak separations for carbonyl signals at approx. 174 ppm and C-2 glycerol signals at approx. 70 ppm, the frequency difference for the two presumed conformations of DPPC is approx. 100 Hz. The NMR time scale for the possible exchange of these two conformations can practically be calculated as $\tau_c = \sqrt{2}/100\pi \cong 5 \cdot 10^{-3}$ s. This is a very slow rate, which is not easy to obtain from broadline NMR studies. In conclusion, at temperatures close to the pretransition temperature of DPPC bilayers, two types of motion would occur. One is associated with the slow exchange of two types of glycerol conformation with an exchange rate of $5 \cdot 10^{-3}$ s, the other is the long axis diffusion of DPPC molecules with a rate of 10^{-5} s.

Finally, the dynamics of the carbonyl group for MAPC and DPPC have been studied by rotating frame relaxation measurements. Due to the lack of a covalent bond proton in the carbonyl group, the implications of the intensity profile detected by us as a function of dipolar contact time is not clear. It has been shown that without proton decoupling, the ^{13}C-labeled carbonyl signal would exhibit a broadened lineshape in comparison with proton decoupling [16]. Therefore, other protons surrounding the carbonyl group can still provide contact channels through the dipolar mechanism. In this respect, interdigitated MAPC bilayers show typical intensity variations which can be simulated by Eqn. 1, but DPPC bilayers show only ^{1}H-^{13}C cross polarization without any $T_{1\rho}$ decay. It is possible that the detectable ^{13}C signal from the carbonyl group are mainly from the L_α phase, which shows a sharp isotopic peak even without magic angle spinning. If this is correct, then the carbonyl group of MAPC is, in contrast to the high mobility of the phosphocholine headgroup, rigid, as implied by relaxation measurements.

In summary, CP/MAS ^{13}C-NMR has been demonstrated to be a useful technique for the study of the packing and the dynamics of aggregated phospholipids in excess water. Conformational-dependent ^{13}C-NMR chemical shifts allows us to compare the packing properties of MAPC molecules in either interdigitated gel state bilayers or fluid state micelles with those of DPPC bilayers. Rotating frame spin-lattice relaxation measurement further suggest a dynamic picture for MAPC interdigitated bilayer which is different from DPPC bilayers at the headgroup, carbonyl group and fatty acyl chain.

Acknowledgements

This work was partly supported by NSC 77-0208-M007-92 and NSC 78-0208-M007-100.

References

1 Wu, W. and Huang, C. (1983) Biochemistry 22, 5068–5073.
2 Jain, M.K., Crecely, R.W., Hille, J.D.R., De Haas, G.H. and Gruner, S.M. (1985) Biochim. Biophys. Acta 813, 68–76.
3 Hui, S.W. and Huang, C. (1986) Biochemistry 25, 1330–1335.
4 Mattai, J. and Shipley, G.G. (1986) Biochim. Biophys. Acta 859, 257–265.
5 Huang, C. and Mason, J.T. (1986) Biochim. Biophys. Acta 864, 423–470.
6 Slater, J.L. and Huang, C. (1988) Prog. Lipid Res. 27, 325–359.
7 Wu, W., Huang, C., Conley, T.G., Martin, R.B. and Levin, I.W. (1982) Biochemistry 21, 5957–5961.
8 McIntosh, T.J., McDaniel, R.V. and Simon, S.A. (1983) Biochim. Biophys. Acta 731, 97–108.
9 Smith, I.C.P., Butler, K.W., Tulloch, A.P., Davis, J.H. and Bloom, M. (1979) FEBS Lett. 100, 57–60.
10 Lin, H.-N. and Huang, C. (1988) Biochim. Biophys. Acta 946, 178–184.
11 Chapman, D., Williams, R.M. and Ladbroode, B.D. (1967) Chem. Phys. Lipids 1, 445–475.
12 Chen, S.C., Sturtevant, J.M. and Gaffney, B.J. (1980) Proc. Natl. Acad. Sci. USA 77, 5060–5063.
13 Wu, W., Chong, P.L.-G. and Huang, C. (1985) Biophys. J. 237–242.
14 Tardieu, A., Luzatti, V. and Reman, F.C. (1973) J. Mol. Biol. 75, 711–733.
15 Janiak, M.J., Small, D.M. and Shipley, G.G. (1979) J. Biol. Chem. 254, 6068–6078.
16 Wittebort, R.J., Schmidt, C.F. and Griffin, R.G. (1981) Biochemistry 20, 4223–4228.
17 Wittebort, R.J., Bume, A., Huang, T.-H., Das Gupta, S.K. and Griffin, R.G. (1982) Biochemistry 21, 3487–3502.
18 Oldfield, E., Bowers, J.L. and Forbes, J. (1987) Biochemistry 26, 6919–6923.
19 Pearson, R.H. and Pascher, I. (1979) Nature 281, 499–501.
20 Pines, A., Gibby, M.G. and Waugh, J.S. (1974) J. Chem. Phys. 56, 1776.
21 Boroske, E. and Trahms, L. (1983) Biophys. J. 42, 275–283.
22 Bartlett, G.R. (1959) J. Biol. Chem. 234, 466–468.
23 Van Echteld, C.J.A., De Kruijff, B., Mandersloot, J.G. and De Gier, J. (1981) Biochim. Biophys. Acta 649, 211–220.

24 Burns, R.A., Jr. and Roberts, M.F. (1980) Biochemistry 19, 3100–3106.
25 Burns, R.A., Jr., Roberts, M.F., Dluhy, R. and Mendelsohn, R. (1982) J. Am. Chem. Soc. 104, 430–438.
26 Balchelor, J.G. and Prestegard, J.H. (1972) Biochem. Biophys. Res. Commun. 48, 70–75.
27 Saitô, H. (1986) Magn. Reson. Chem. 24, 835–852.
28 Lugtinburg, J., Mathies, R.A., Griffin, R.G. and Herzfeld, J. (1988) Trends. Biochem. Sci. 13, 388–393.
29 Seelig, J. and Seelig, A. (1980) Q. Rev. Biophys. 13, 19–61.
30 Bueldt, G. and Wohlgemuth, R. (1981) J. Membr. Biol. 58, 81–100.
31 Davis, J.H. (1983) Biochim. Biophys. Acta 737, 117–171.
32 Zasadzinski, J.A.N. (1988) Biochim. Biophys. Acta 946, 235–243.
33 Hatta, I. and Tsuchida, K. (1988) Biochim. Biophys. Acta 945, 73–80.
34 Wu, W. (1983) Ph.D. Thesis, University of Virginia, Charlottesville.
35 Philipis, M.C., Williams, R.M. and Chapman, D. (1969) Chem. Phys. Lipids 3, 324–344.
36 Nagle, J.F. (1980) Annu. Rev. Phys. Chem. 31, 159–195.
37 Chendy, V.B. and Grant, D.M. (1967) J. Am. Chem. Soc. 89, 5319–5327.
38 Dill, K.A. and Flory, P. (1981) Proc. Natl. Acad. Sci. USA 78, 676.
39 Seelig, J. (1977) Q. Rev. Biophys. 10, 353–418.
40 Walderhaug, H., Soderman, O. and Stilbs, P. (1984) J. Phys. Chem. 88, 1655–1662.
41 Marsh, D. (1980) Biochemistry 19, 1632–1637.
42 Ruocco, M.J., Siminovitch, D.J. and Griffin, R.G. (1985) Biochemistry 24, 2406–2411.
43 Ruocco, H.J., Makriyannis, A., Siminovitch, D.J. and Griffin, R.G. (1985) Biochemistry 24, 4844–4851.
44 Wu, W., Stephenson, F.A., Mason, J.T. and Huang, C. (1984) Lipids 19, 68–71.
45 Blume, A., Rice, D.M., Wittebort, R.J. and Griffin, R.G. (1982) Biochemistry 21, 6220–6230.
46 Mason, J.T., Huang, C. and Biltonen, R.L. (1983) Biochemistry 22, 2013–2018.